Electronic Supplementary Information

Hybrid perovskite crystallization from binary solvent mixtures: interplay of evaporation rate and binding strength of solvents

Oleksandra Shargaieva, [a] Hampus Näsström, [a] Joel A. Smith, [b] Daniel Többens, [c] Rahim Munir, [d] and Eva L. Unger [a]

[a.] *Helmholtz-Zentrum Berlin für Materialien und Energie GmbH, Young Investigator Group 'Hybrid Materials Formation and Scaling', Kekulestr. 5, 12489 Berlin (Germany).*

[b.] *University of Sheffield, Department of Physics & Astronomy, Sheffield, S3 7RH, U.K.*

[c.] *Helmholtz-Zentrum Berlin für Materialien und Energie GmbH, Department of Structure and Dynamics of Energy Materials, Albert-Einstein-Str. 15, 12489 Berlin (Germany).*

[d.] *University of Calgary, Chemistry department, 2500 University Dr NW, AB T2N 4V8, Calgary, Canada*

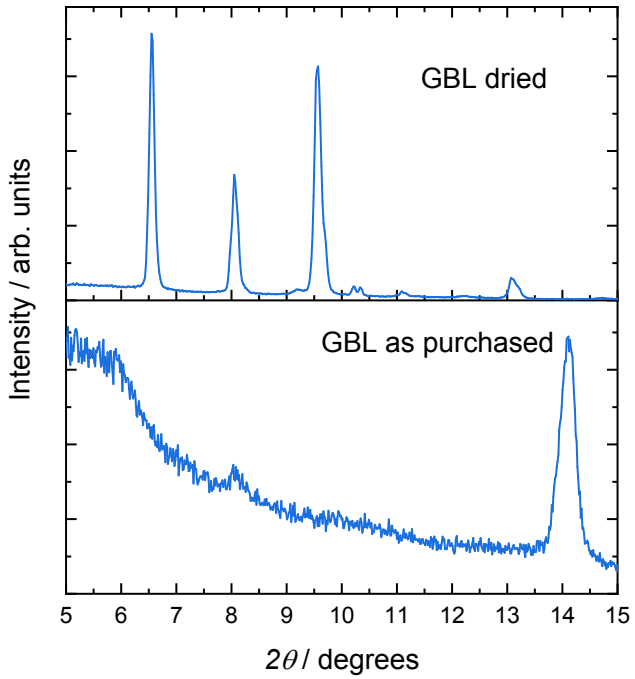

Figure S1. Diffraction patterns of the intermediate phases formed from solutions of $MAPbI_3$ in GBL dried over molecular sieves and as-purchased anhydrous solvent.

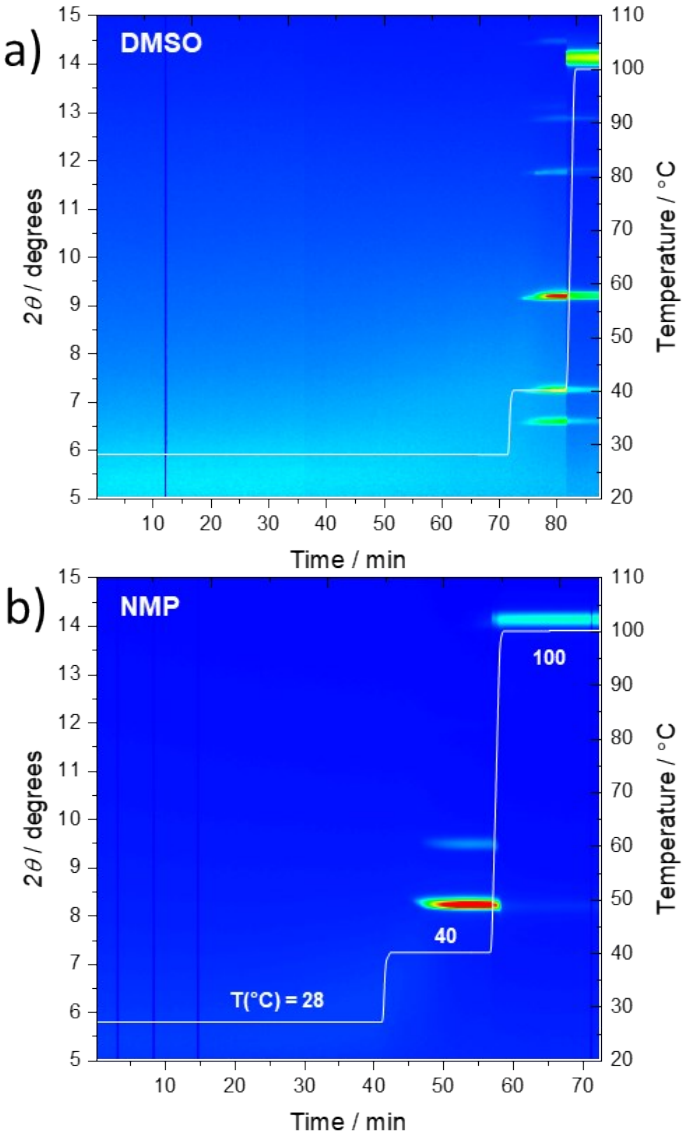

Figure S2 2D contour plots of the azimuthally integrated GIWAXS patterns of $MAPbI_3$ solutions in a) DMSO and b) NMP as a function of drying time. The temperature regimes used for the experiments are indicated by the white lines and shown on the right axis.

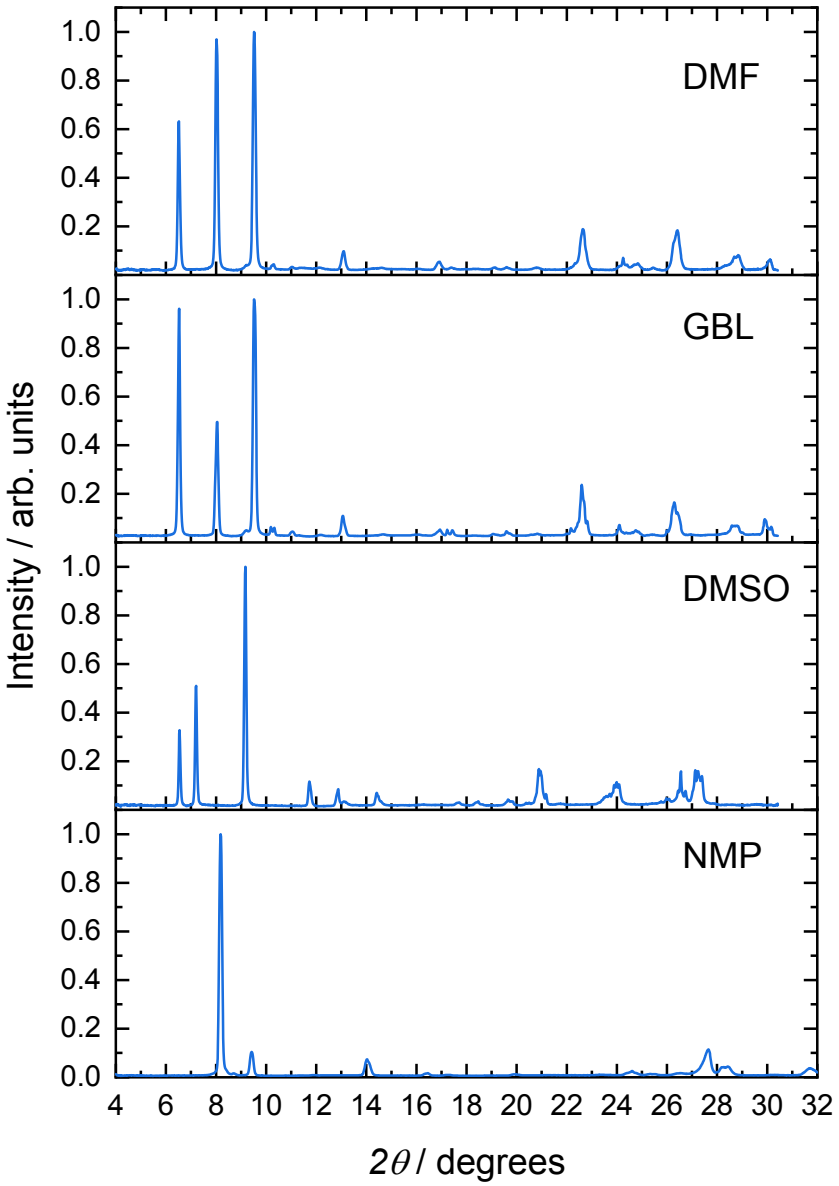

Figure S3. Diffraction patterns of the intermediate phases from DMF, GBL, DMSO, and NMP $MAPbI_3$ solutions.

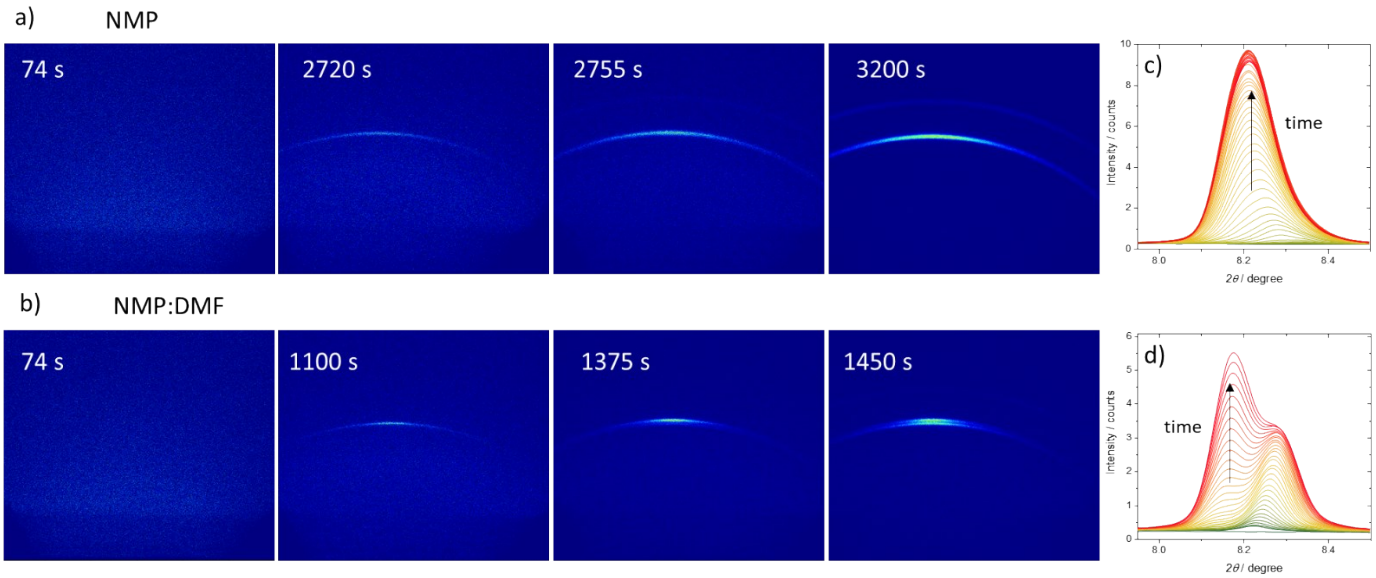

Figure S4. GIWAXS detector images of $MAPbI_3$ solutions coated from a) NMP and b) DMF:NMP 50:50%v/v as a function of time at 28 °C. Integrated GIWAXS patterns of the same solutions as a function of time are shown in c) and d) respectively.

Table S1. Experimental time of onset of crystallization for $MAPbI_3$ solutions with binary solvent mixtures, calculated evaporation rates (R_{Evap}) at 28 °C and number of solvent molecules A and B at the beginning of the experiment and the onset of crystallization.

Solvent mixture A : B	***Time until crystallization / min***	***R_{Evap} / mol/m s at 28 °C***	***N_A:N_B at the beginning of experiment***	***N_A:N_B at the onset of crystallization***
DMF : DMSO	20.4	1.96×10^{-6}	6.5 : 7.0	0.5 : 4.7
DMF : NMP	21.2	2.20×10^{-6}	6.5 : 5.2	0.3 : 3.1
DMSO : GBL	23.5	1.41×10^{-6}	7.0 : 6.5	4.4 : 0.9
NMP : GBL	24.3	1.57×10^{-6}	5.2 : 6.5	2.3 : 0.3
DMF : GBL	8.5	2.93×10^{-6}	6.5 : 6.5	2.2 : 3.2
DMSO : NMP	32	5.60×10^{-7}	7.0 : 5.2	3.1 : 2.1

Pure solvent	***Time until crystallization / min***	***R_{Evap} / mol/m s at 28 °C***	***N_A at the beginning of experiment***	***N_A at the onset of crystallization***
DMF	3.75	3.51×10^{-6}	12.9	8.8
GBL	5.75	2.36×10^{-6}	13	8.9
NMP	46.18*	5.93×10^{-7}	10.36	2.5
DMSO	74.93*	5.36×10^{-7}	14.15	2.5

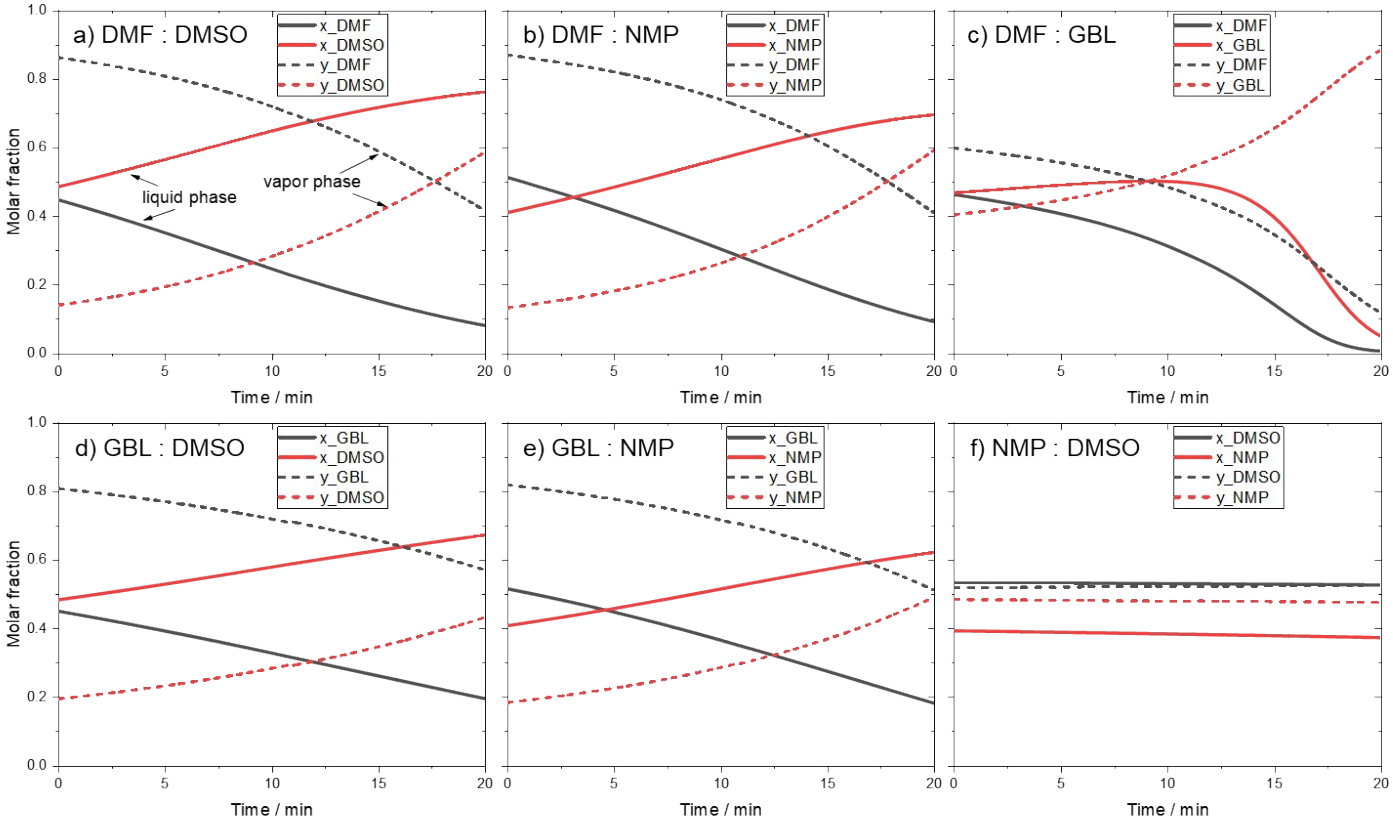

Figure S5. Composition of vapor (y) and liquid (x) phases as a function of time for binary mixtures (50:50 %v/v) of solvents a) DMF:DMSO, b) DMF:NMP, c) DMF:GBL, d) GBL:DMSO, e) GBL:NMP, and f) NMP:DMSO.

a) DMF

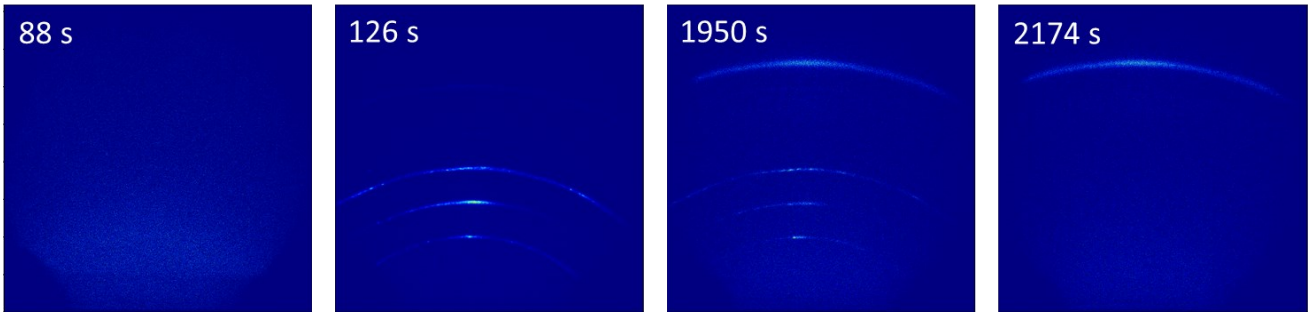

b) DMSO

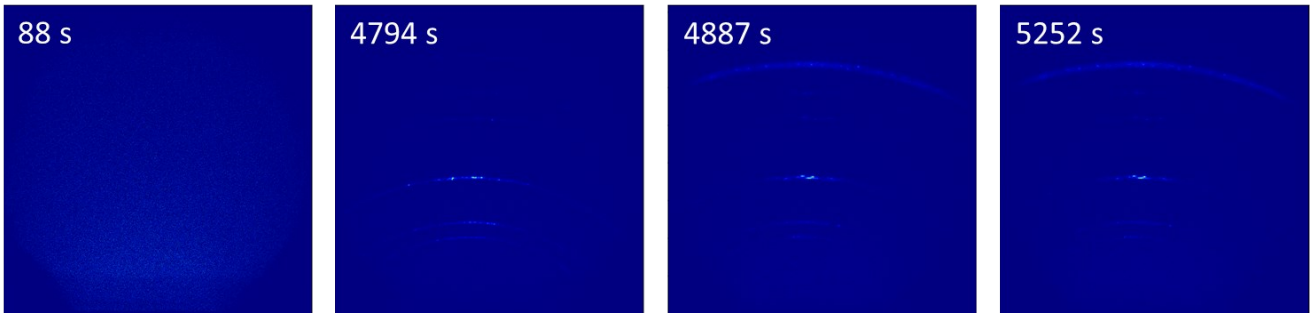

c) GBL

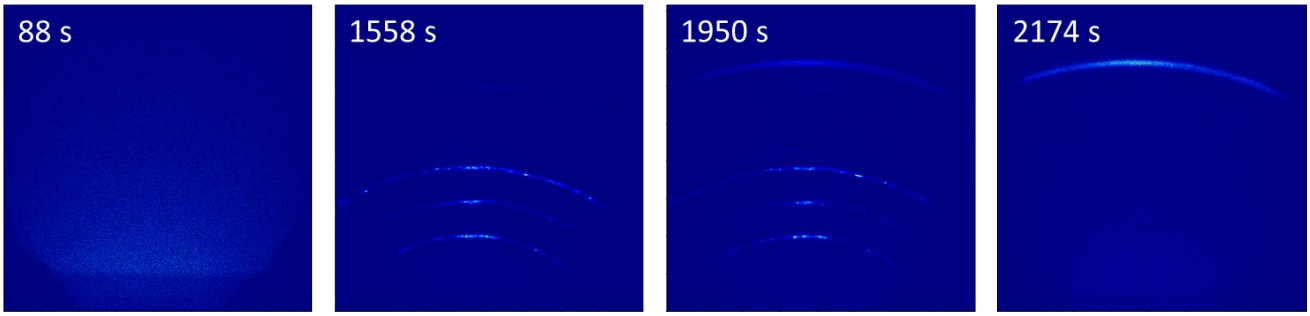

Figure S6. GIWAXS detector images of $MAPbI_3$ solutions coated from a) DMF, b) DMSO, and c) GBL as a function of time at 28, 40, and 100 °C.

a) DMF : DMSO

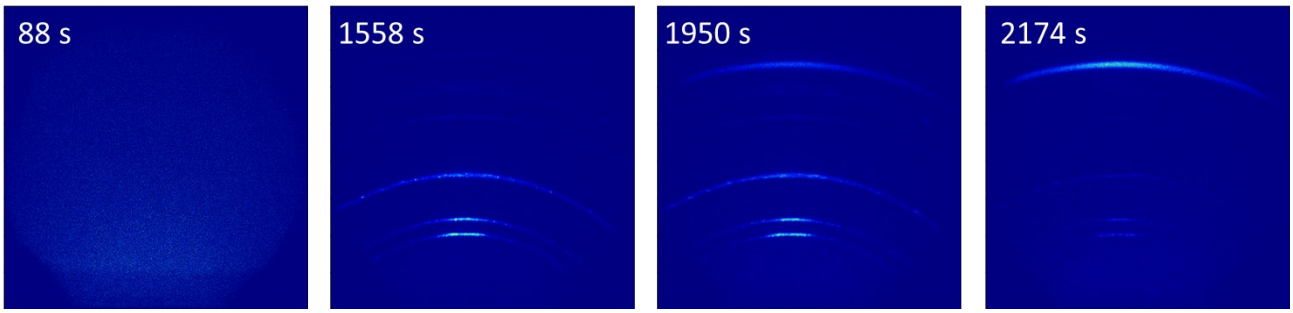

b) GBL : DMSO

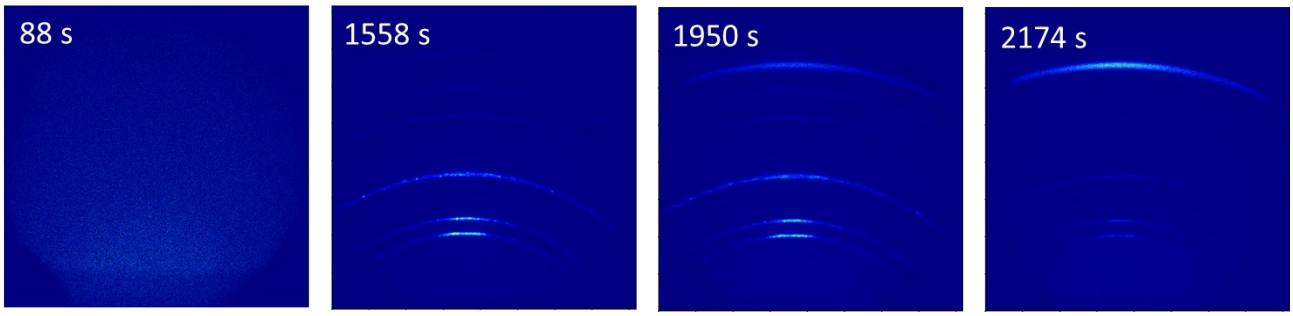

c) GBL : NMP

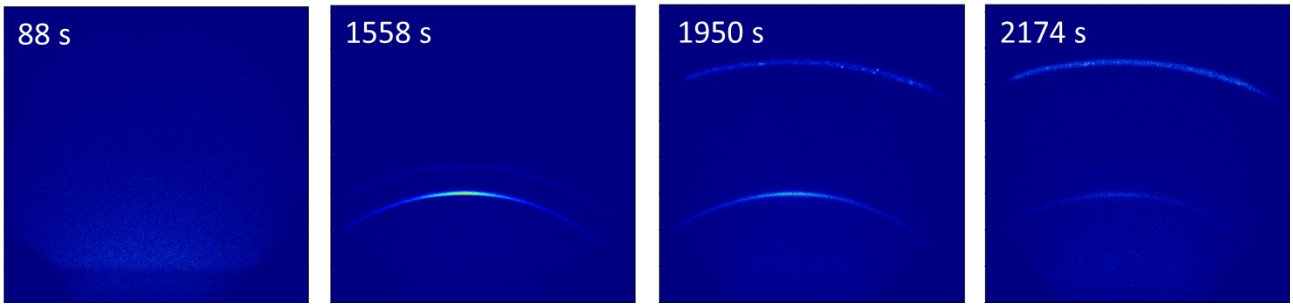

d) GBL : DMF

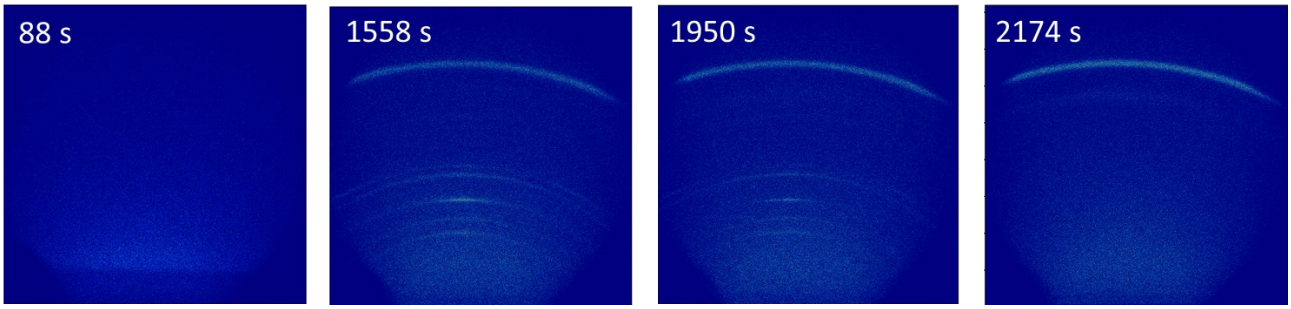

e) NMP : DMSO

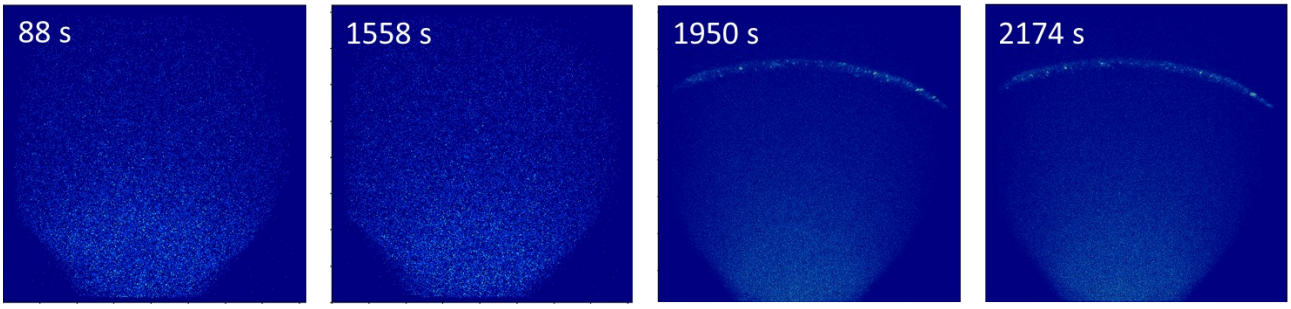

Figure S7. GIWAXS detector images of $MAPbI_3$ solutions coated from a) DMF:DMSO, b) GBL:DMSO, c) GBL:NMP, d) GBL:DMF, and e) NMP:DMSO (50:50%v/v) as a function of time at 28, 40, and 100 °C.

Evaporation model

The rate of solvent evaporation, R_{evap}, for a given solvent was calculated using equation (1).

$$Revap = K_m L \frac{P_v}{R T} \quad , (1)$$

where K_m is the mass transfer coefficient, L is the length (or square root of the area $\sqrt{A}$) of the liquid film, P_v is vapor pressure of the solvent, R – the gas constant, T – the temperature in K.

In order to calculate the evaporation rates at given conditions, the temperature-dependent values of $P_{v,}$ and the mass transfer coefficient K_m need to be found. Temperature-dependent curves for the vapor pressure of the solvents were calculated using the Clausius-Clapeyron equation and tabular values for P_v at different temperatures.[1] The mass transfer coefficient (K_m) was calculated using the Sherwood number, *Sh*, which can be calculated from equation (2) using Reynolds and Schmidt numbers:[2]

$$Sh = \frac{K_m L}{D} = 0.664 \times \sqrt{Re} \times \sqrt[3]{Sc} \quad , (2)$$

where D is the diffusion coefficient of solvent in nitrogen, *Re* – Reynolds number, *Sc* – Schmidt number.

The equation (2) can be used only for systems with laminar flow conditions determined by small Reynolds numbers and slow flow. Schmidt and Reynolds numbers can be calculated according to the equation (3) and (4) respectively:

$$Sc = \frac{\eta}{D} \quad , (3)$$

where η is the kinematic viscosity of nitrogen gas[3] and

$$Re = \frac{U \times L}{\eta} \quad , (4)$$

where U is air velocity.

For calculation of both the mass transfer coefficient and Schmidt number, the temperature-dependent diffusion coefficient, D, needs to be calculated for the diffusion of solvent molecules (A) through nitrogen gas (B) at the boundary layer at given conditions. The diffusion coefficients were calculated using Hirschfelder, Bird, and Spotz equation (5) based on Chapman–Enskog theory:[4,5]

$$D = \frac{\alpha T^{3/2} \sqrt{\frac{1}{M_w(A)} + \frac{1}{M_w(B)}}}{P \sigma^2 \Omega} \quad , (5)$$

Where α is a constant (α = 0.001858), M_w is the molar weight of the components, P is atmospheric pressure, Ω is the temperature-dependent collision integral for molecular diffusion and σ is the Lennard-Jones average collision diameter.

For estimating the diffusion coefficient for binary gas mixtures containing polar compounds, the collision integral can be calculated using the equation (6):

$$\Omega_D = \Omega_D^0 + \frac{0.19 \delta_{AB}^2}{T^*} \quad , (6)$$

The reference collision integral, Ω_D^0, is estimated by (7):

$$\Omega_D^0 = \frac{A}{(T^*)^B} + \frac{C}{\exp(D \times T^*)} + \frac{E}{exp(F \times T^*)} + \frac{G}{\exp(H \times T^*)}, \quad (7)$$

where *A*=1.06036; *B*= 0.15610; *C*= 0.19300; *D*= 0.47635; *E* = 1.03587; *F* = 1.52996; *G* = 1.76474; *H*=3.89411 are Neufeld constants and T^* is the reduced temperature given by equation (8):[6]

$$T^* = \frac{kT}{\epsilon_{AB}}, \quad (8)$$

The energy of molecular interaction for the binary system *A* and *B*, ϵ_{AB}, is calculated according to (9):

$$\epsilon_{AB} = \sqrt{\epsilon_A \times \epsilon_B}, \quad (9)$$

The energy of molecular interaction for pure components, $\frac{\epsilon_A}{k}$, can be found using tabulated Lennard -Jones force constants or calculated using equation (10)[7]

$$\frac{\epsilon_A}{k} = 1.18\,(1 + 1.3\delta_A^2)T_b, \quad (10)$$

Where T_b is the boiling point in Kelvin. Using the Brokaw relation, this equation can be modified for polar components by introducing the dipole moment of a molecule, μ_p (11):[8]

$$\delta_{AB} = \sqrt{\delta_A \times \delta_B}, \text{ where } \delta = \frac{1.94 \times 10^3 \times \mu_p^2}{V_b T_b}, \quad (11)$$

Where V_b is the molar volume at the boiling point. The average collision diameter of solvent and nitrogen gas can be estimated using equation (12):

$$\sigma_{AB} = \sqrt{\sigma_A \times \sigma_B}, \quad (12)$$

where each component's characteristic size is calculated by equation (13):

$$\sigma_A = \sqrt[3]{\frac{1.585 V_b}{1 + 1.3\delta_A^2}}, \quad (13)$$

Combining equations (6) – (13), the diffusion coefficient can be calculated at given experimental conditions. The vapor pressure of the solution was calculated according to Raoult's law (14):

$$P_A = p_A^0 x_A, \quad (14)$$

where, P_A is the vapor pressure of solvent A over the solution, p_A^0 is the vapor pressure of solvent A and x_A is the molar fraction of solvent A. Precursor salts are considered non-volatile and do not interact with the solvent. In reality, the coordination of solvent to precursor molecules is not negligible. However, it is possible to assume that in the solutions with a large excess of solvent, free non-coordinated solvent evaporates at the beginning of the experiment. In a mixture of two components A and B, the total vapor pressure P of a solution can be calculated according to (15):

$$P = P_A + P_B = p_A^0 x_A + p_B^0 x_B, \quad (15)$$

Using the diffusion coefficient, mass transfer coefficient, and the vapor pressure, the evaporation rate can be calculated according to (1). Since the evaporation rate is proportional to the vapor pressure and the vapor pressure depends on the composition of the film, the amount of solvent at a given time, v(t + Δt), was calculated by numerically solving the coupled difference equation (16) with a time step, Δt, of 1 s.

$$\begin{cases} v_A(t+\Delta t) = v_A(t) - R_A^{Evap}(T) \cdot L \cdot \dfrac{v_A(t)}{v_A(t)+v_B(t)+v_{Pero}} \cdot \Delta t, \\ v_B(t+\Delta t) = v_B(t) - R_B^{Evap}(T) \cdot L \cdot \dfrac{v_B(t)}{v_A(t)+v_B(t)+v_{Pero}} \cdot \Delta t, \end{cases} \quad (16)$$

In the mixture of solvents, the evaporation rate of each solvent component depends on the amount of the component in the mixture and its vapor pressure. Therefore, the Konovalov-Gibbs rule was used for calculation of the composition of the vapor and liquid phase (17):

$$y_A = \frac{P_A}{P} = \frac{p_A^0 x_A}{p_A^0 x_A + p_B^0 x_B}, \quad (17)$$

where *y* is the molar fraction of a component in the vapor phase and *x* is the molar fraction of a component in the liquid phase. The change in the respective volumes of solvents was calculated using coupled ordinary differential equations for two components.

It is important to note that this model can be used for calculation of evaporation rates of liquid films deposited by "static" deposition methods such as blade-coating, slot-die, and inkjet printing, where the solvent evaporation is mainly observed after the deposition and determined by the physical and chemical properties of the solvent and e.g. gas flow. In the case of "dynamic" deposition methods such as spin-coating, an additional solvent evaporation needs to be considered due to a high rate of solvent vapor removal from the boundary layer during rotation.

References:

1 J. Rumble, Ed., *Handbook of Chemistry and Physics*, CRC Press, 100th edn., 2019.

2 T. K. Sherwood, R. L. Pigford and C. R. Wilke, *Mass transfer*, McGraw-Hill Book Company, 1975.

3 Engineering ToolBox, Nitrogen - Dynamic and Kinematic Viscosity, https://www.engineeringtoolbox.com/nitrogen-N2-dynamic-kinematic-viscosity-temperature-pressure-d_2067.html, (accessed 15 June 2020).

4 J. R. Welty, G. L. Rorrer and D. G. Foster, *Fundamentals of momentum, heat and mass transfer*, Wiley, 6th edn., 2014.

5 J. O. Hirschfelder, R. Byron Bird and E. L. Spotz, *Chem. Rev.*, 1949, **44**, 205–231.

6 P. D. Neufeld, A. R. Janzen and R. A. Aziz, *J. Chem. Phys.*, 1972, **57**, 1100–1102.

7 E. Wilhelm and R. Battino, *J. Chem. Phys.*, 1971, **55**, 4012–4017.

8 R. S. Brokaw, *J. Chem. Phys.*, 1958, **29**, 391–397.